

Linköping University Post Print

Electronic structure of Ge(111)c(2x8): STM, angle-resolved photoemission, and theory

Ivy Razado, Jiangping He, Hanmin Zhang, Göran Hansson and Roger Uhrberg

N.B.: When citing this work, cite the original article.

Original Publication:

Ivy Razado, Jiangping He, Hanmin Zhang, Göran Hansson and Roger Uhrberg, Electronic structure of Ge(111)c(2x8): STM, angle-resolved photoemission, and theory, 2009, PHYSICAL REVIEW B, (79), 20, 205410.

<http://dx.doi.org/10.1103/PhysRevB.79.205410>

Copyright: American Physical Society

<http://www.aps.org/>

Postprint available at: Linköping University Electronic Press

<http://urn.kb.se/resolve?urn=urn:nbn:se:liu:diva-19417>

Electronic structure of Ge(111) $c(2\times 8)$: STM, angle-resolved photoemission, and theory

I. Razado-Colambo, Jiangping He,^{*} H. M. Zhang,[†] G. V. Hansson, and R. I. G. Uhrberg
Department of Physics, Chemistry, and Biology, Linköping University, S-581 83 Linköping, Sweden
 (Received 2 December 2008; revised manuscript received 17 April 2009; published 14 May 2009)

The surface electronic structure of Ge(111) $c(2\times 8)$ was studied by experimental techniques [low-energy electron diffraction, scanning tunneling microscopy (STM), and angle-resolved photoelectron spectroscopy (ARPES)] and theoretical band-structure calculations. Bias-dependent STM images exhibit two different types of adatoms (A_T, A_R) and rest atoms (R_T, R_R) confirming the presence of asymmetries within the $c(2\times 8)$ cell. The ARPES study resulted in a more detailed picture of the surface electronic structure of the Ge(111) $c(2\times 8)$ surface compared to earlier studies. The energy dispersion curves showed the presence of seven surface bands labeled A1, A2, A2', A3, A4, A4', and A5. The experimental surface bands were compared to the calculated band structure of the full $c(2\times 8)$ unit cell. The most important results are (i) we have identified a split surface-state band in the photoemission data that matches a split between R_T and R_R derived rest atom bands in the calculated surface band structure. This allows us to identify the upper A2 band with the R_R and the lower A2' band with the R_T rest atoms. (ii) The uppermost highly dispersive band (A1) originates from states below the adatom and rest atom layers and should not be confused with rest atom bands A2 and A2'. (iii) The bias-dependent changes in the adatom/rest atom contrast in the experimental STM images were closely reproduced by simulated STM images generated from the calculated electronic structure. (iv) A split was observed in the back-bond derived surface band at higher emission angles (A4 and A4').

DOI: [10.1103/PhysRevB.79.205410](https://doi.org/10.1103/PhysRevB.79.205410)

PACS number(s): 68.35.B-, 68.37.Ef, 79.60.-i

I. INTRODUCTION

Studies of the electronic structure of semiconductor surfaces such as Si and Ge have caught a lot of attention during several decades. The (111) surfaces are particularly interesting due to the complex reconstructions formed upon annealing. The electronic structure of Si(111) 7×7 is more well established than that of the Ge(111) $c(2\times 8)$ surface. Though there have been several experimental and theoretical studies performed on the Ge(111) $c(2\times 8)$ surface to obtain the electronic structure, there are still unresolved issues regarding the origins of some of the surface-state bands. Theoretical surface band-structure calculations are difficult to carry out since Ge(111) $c(2\times 8)$ has quite a large unit cell. The aim of this paper is to obtain a detailed picture of the electronic structure of the Ge(111) $c(2\times 8)$ surface by combining angle-resolved photoelectron spectroscopy (ARPES), scanning tunneling microscopy (STM), and theoretical surface band-structure calculations.

The atomic structure of the Ge(111) $c(2\times 8)$ surface is already well established. Chadi and Chiang¹ were the first to propose that the Ge(111) surface had a $c(2\times 8)$ instead of a 2×8 unit cell, which explained the incomplete set of eighth-order reflections in the low-energy electron diffraction (LEED) pattern. A few years later, Phaneuf and Webb² observed a small intensity of the fourth-order LEED spots that implies asymmetries in the unit cell. Figure 1(a) shows the accepted model of the $c(2\times 8)$ structure consisting of one-fourth monolayer (ML) of adatoms.^{3,4} Each adatom bonds to three atoms in the first full layer, thus saturating three-fourths of the surface dangling bonds. The surface is further stabilized by a charge transfer from the one-fourth ML of adatom dangling bonds to the remaining one-fourth ML of unsaturated dangling bonds on the rest atoms (atoms of the first layer not bonding to adatoms). This leads to filled and empty

surface-state bands mostly located at the rest atoms and adatoms, respectively. The $c(2\times 8)$ structure consists of 2×2 and $c(2\times 4)$ subunit cells leading to two types of rest atoms (adatoms) with different local environments. One type of rest atom, R_T (adatom, A_T) is symmetrically surrounded by three adatoms (rest atoms) forming a triangle, and one rest atom, R_R (adatom, A_R) is asymmetrically surrounded by four adatoms (rest atoms) forming a rectangle as shown in Fig. 1(a). Differences in the structure of the 2×2 and $c(2\times 4)$ subunits of the $c(2\times 8)$ unit cell were found based on the theoretical calculations of Takeuchi *et al.*⁵ The two rest atoms showed a

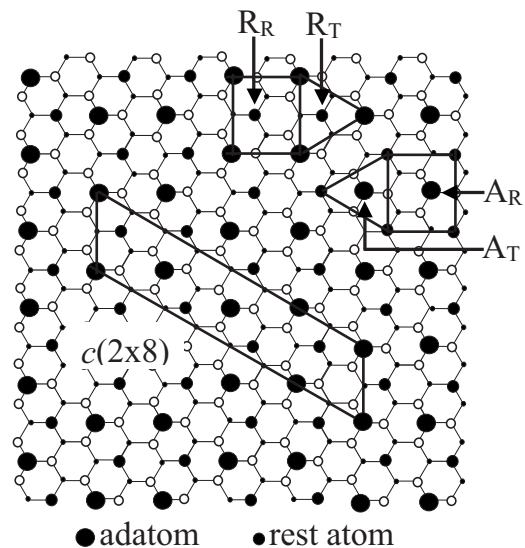


FIG. 1. Ge(111) $c(2\times 8)$ model. The large solid circles are the adatoms, and the smaller solid circles are rest atoms. There are two kinds of rest atoms (adatoms). One is symmetrically surrounded by three adatoms (rest atoms), R_T (A_T), and the other is asymmetrically surrounded by four adatoms (rest atoms), R_R (A_R).

height difference on the order of 0.03 Å and in-plane asymmetries on the order of 0.1 Å while smaller asymmetries were found for the adatoms. These results are consistent with the LEED pattern observed by Phaneuf and Webb² which showed a nonzero intensity of the fourth-order spots contrary to what is expected for a perfectly symmetric $c(2\times 8)$ cell.

The adatom model of the Ge(111) $c(2\times 8)$ surface is also supported by STM images obtained by several groups. In the STM study by Becker *et al.*,³ the images showed protrusions matching either the rest atoms, when probing the filled states, or the adatoms, when probing the empty states, but not simultaneously. This suggested that there is a complete electron transfer from the adatoms to the rest atoms. An STM study by Hirschorn *et al.*⁴ confirmed that the simple adatom model is valid. The rest atoms were the dominant features in the images taken with a negative sample bias. However, the adatom contribution became noticeable at a smaller absolute value of the negative bias. This suggests that the electron transfer from the adatoms to the rest atoms is not actually complete. At positive sample bias, the adatoms were the dominant features. In this paper, we present a detailed account of the adatom and rest atom contributions to the STM images for various sample biases corresponding to both empty and filled states.

Since the Ge(111) $c(2\times 8)$ surface has a large unit cell, band-structure calculations are quite complicated. As a consequence of this, there is no surface band structure of the full $c(2\times 8)$ cell to be found in the literature. Experimentally, several studies have been performed in order to obtain dispersion curves of the surface states. In the ARPES study by Bringans and Höchst,⁶ two distinct surface states were observed at 0.8 and 1.4 eV below the top of the valence band. These two peaks disappeared after hydrogen adsorption, which indicates that they both correspond to emission from surface states. Angle-resolved ultraviolet photoemission measurements were also performed by Yokotsuka *et al.*,⁷ and they found two peaks at ~ -0.8 and ~ -1.4 eV relative to the Fermi level (E_F) that they referred to as dangling- and back-bond surface states. These previous photoemission studies used a photon energy of 21.2 eV. Nicholls *et al.*⁸ used a lower photon energy (10.2 eV) and observed additional surface structures dispersing between the previously observed bands. The photoemission study by Bringans *et al.*⁹ revealed the presence of 2×2 subunits on the $c(2\times 8)$ surface based on the symmetry of the surface-state dispersions. Further, they found two strong surface states in the gap of the projected band structure that were split by about 0.7 eV. Photoemission data from the Ge(111) $c(2\times 8)$ surface by Aarts *et al.*¹⁰ showed the existence of two surface-state bands (S1 and S2) with dangling-bond character and an apparent (1×1) periodicity. The top of the S1 band was about 0.15 eV below the valence band maximum (VBM), and the S2 band was positioned at ~ 0.65 eV. S1 could not be attributed to partly filled adatom dangling bonds, as in the case of Si(111) 7×7 , since based on the existing adatom model for Ge(111) $c(2\times 8)$ there is an equal number of adatoms and rest atoms that leads to empty adatom states. It was therefore concluded that S1 could not be fully explained within the existing models. S2 was identified as originating from the rest atoms partly based on the identification of a similar sur-

face state on Si(111) 7×7 based on STM measurements by Hamers *et al.*¹¹ Another two dispersive surface features, labeled S3 and S4, were identified in the study by Aarts *et al.*¹⁰ and were assigned to “adatom structures” on the surface.

In this paper we present additional experimental and theoretical results from which we have derived a detailed picture of the origins of the surface states on Ge(111) $c(2\times 8)$. The problem with the identification of the S1 band discussed by Arts *et al.*¹⁰ has been resolved. We show that the S1 band is actually a combination of a band originating from states below the uppermost surface layer near the center of the surface Brillouin zone (SBZ) while the outer part corresponds to rest atom states. We have further identified a split between the states on the two types of rest atoms. This split is nicely reproduced in the surface band-structure calculations. Our bias-dependent STM images provide important information on the two types of adatoms and rest atoms that are present on the $c(2\times 8)$ surface. The variation in the adatom/rest atom contrast in the experimental images is closely reproduced in the simulated bias-dependent STM images derived from the electronic structure that we have calculated using the full $c(2\times 8)$ unit cell.

II. EXPERIMENTAL AND THEORETICAL DETAILS

The photoemission experiments were performed at beam line 33 at the Max-lab synchrotron radiation facility in Lund, Sweden. The angle-resolved valence band spectra were obtained with a total-energy resolution of ~ 70 meV and an angular resolution of $\pm 2^\circ$. An Sb-doped ($\rho=3 \Omega \text{ cm}$) Ge(111) sample was cleaned by ion sputtering (Ar^+ , 0.5 kV). Thermal annealing for several minutes at $\sim 600^\circ \text{C}$ was done in order to recover the crystalline structure. The procedure resulted in a well-ordered surface as evidenced by sharp $c(2\times 8)$ LEED spots. After the sample cleaning procedure, the sample was immediately transferred to the photoemission chamber of the ultrahigh vacuum system for measurements.

The STM measurements were carried out in a homebuilt UHV STM/molecular-beam epitaxy (MBE) system at Linköping University, Sweden.¹² It was equipped with LEED and quadrupole mass spectroscopy (QMS). The Ge(111) sample was prepared in a similar manner as in the photoemission studies. All images were recorded at room temperature in constant-current mode using a cut Pt/Ir tip.

The theoretical calculations reported in this paper were carried out using the *ab initio* total-energy and molecular dynamics program Vienna *ab initio* simulation package (VASP) which is based on the density functional theory (DFT) pseudopotential plane wave method.^{13–15} The calculations were performed using the projector augmented wave (PAW) potentials^{16,17} in the generalized gradient approximation (GGA), included in the VASP code.^{13–15} In the PAW potential of germanium the $3d^{10}4s^24p^2$ states were treated as valence states. The initial surface structure was based on the results of Ref. 18. A germanium lattice constant of 5.765 Å was obtained using the same method and PAW potential as for the Ge(111) $c(2\times 8)$ surface relaxation. The Kohn-Sham equations were solved using ten special k points in the irreducible symmetry element of the surface Brillouin zone (SBZ) of the

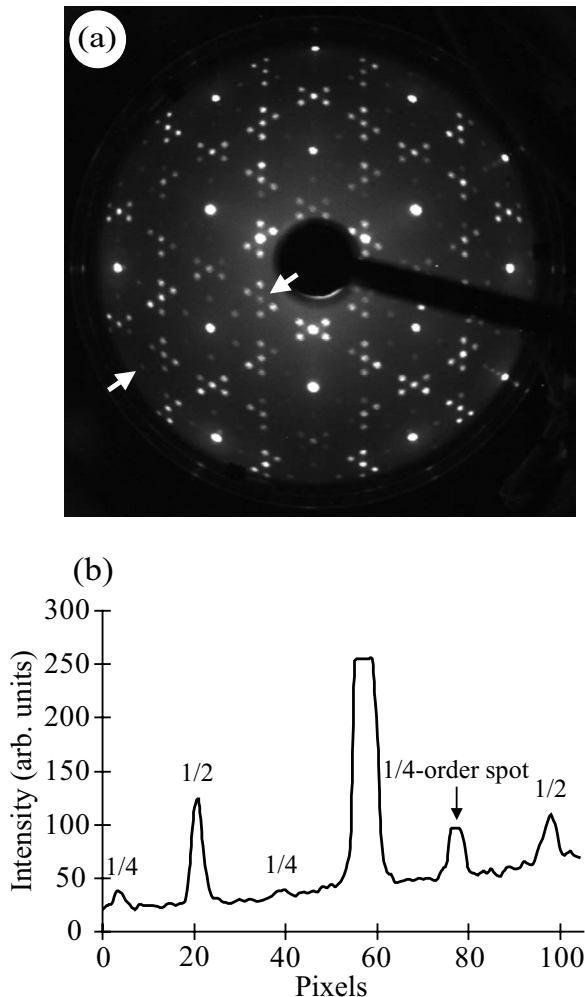


FIG. 2. (a) LEED pattern of the Ge(111) $c(2\times 8)$ surface recorded with a primary electron energy of 110 eV at a temperature of 100 K. (b) Intensity profile of the diffraction spots along a line between the two arrows in Fig. 2(a). One of the fourth-order diffraction spots is well defined as revealed by the line profile.

$c(2\times 8)$ surface unit cell and employing an energy cutoff of ~ 22 Rydbergs. The $c(2\times 8)$ surface was modeled by a periodic slab composed of eight layers of germanium, plus eight hydrogen atoms to saturate the dangling bonds of the bottom layer germanium atoms, and a vacuum region of ~ 11.5 Å. All germanium atoms, except the bottom four layers that were held at bulk positions, were relaxed until the residual force components became smaller than 0.02 eV/Å. Using the relaxed geometry, the constant-current STM images were calculated within the Tersoff-Hamann approximation.¹⁹ The surface band character was based on the calculation of the partial (band decomposed) charge density.

III. RESULTS

A. LEED and STM results

Figure 2(a) shows the LEED pattern of the clean surface. The sharp $c(2\times 8)$ diffraction spots confirm that the surface has a well-ordered periodicity. The half-order and eighth-

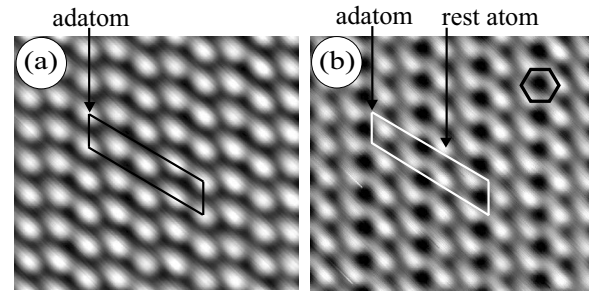


FIG. 3. (a) and (b) are empty and filled-state STM images of the Ge(111) $c(2\times 8)$ surface. The images were recorded at a tip bias of -1.2 and $+1.2$ V, respectively, and a tunneling current of 0.1 nA. Image sizes are 61×67 Å².

order spots can be clearly observed in the LEED pattern. This result is consistent with the theoretical study by Chadi and Chiang¹ who suggested that the surface has a $c(2\times 8)$ instead of a simple 2×8 unit cell. Note that the LEED pattern shows the weak fourth-order spots discussed in Refs. 2 and 5. A line profile through the diffraction spots [between the two arrows in Fig. 2(a)] is presented in Fig. 2(b). The presence of the fourth-order spots indicates asymmetries in the surface unit cell.

The empty-state STM image of the clean surface in Fig. 3(a) shows only the adatoms. This is in agreement with previous STM studies^{3,4} and theoretical results by Klitsner and Nelson²⁰ that the primary unoccupied surface states are strongly localized on the adatom sites. The $c(2\times 8)$ unit cell is also indicated in the image. The position of the unit cell with respect to the adatoms is the same as in Fig. 1. Figure 3(b) shows a filled-state STM image where the primary occupied surface state is predominantly localized on the rest atom sites. The calculations by Klitsner and Nelson²⁰ also revealed that other occupied states exist contributing to the adatom surface charge density. Since the adatom is physically higher than the rest atom, both adatoms and rest atoms are observed in the filled-state image resulting in the appearance of a structure with interconnected sixfold rings as indicated by the hexagon in Fig. 3(b).

Figure 4 shows STM images of the Ge(111) $c(2\times 8)$ surface using different tip biases and the corresponding line profiles across the adatoms and the rest atoms. The solid white arrows indicate the paths along which the adatom profiles were obtained (black curves), while the dashed arrows have the same meaning but for the rest atom profiles (gray curves). The larger circles denote the adatom positions, while the smaller circles correspond to rest atom positions. In the empty-state STM images ranging from -0.4 to -1.5 V, the dominant features are the adatoms. At tip voltages ranging from -0.4 to -0.8 V, the adatoms surrounded by three rest atoms (A_T) in the triangular subunit cell appear slightly higher than the adatoms surrounded by four rest atoms (A_R). Going from -0.8 to -1.0 V, there is a reversal in the brightness of the two types of adatoms. The A_T type of adatom becomes less bright than the A_R type.

At lower positive tip voltages ($+0.4$ and $+0.5$ V), the adatoms dominate the STM images. The rest atoms begin to be visible at $+0.6$ V. At $+0.7$ V, the R_R rest atoms have be-

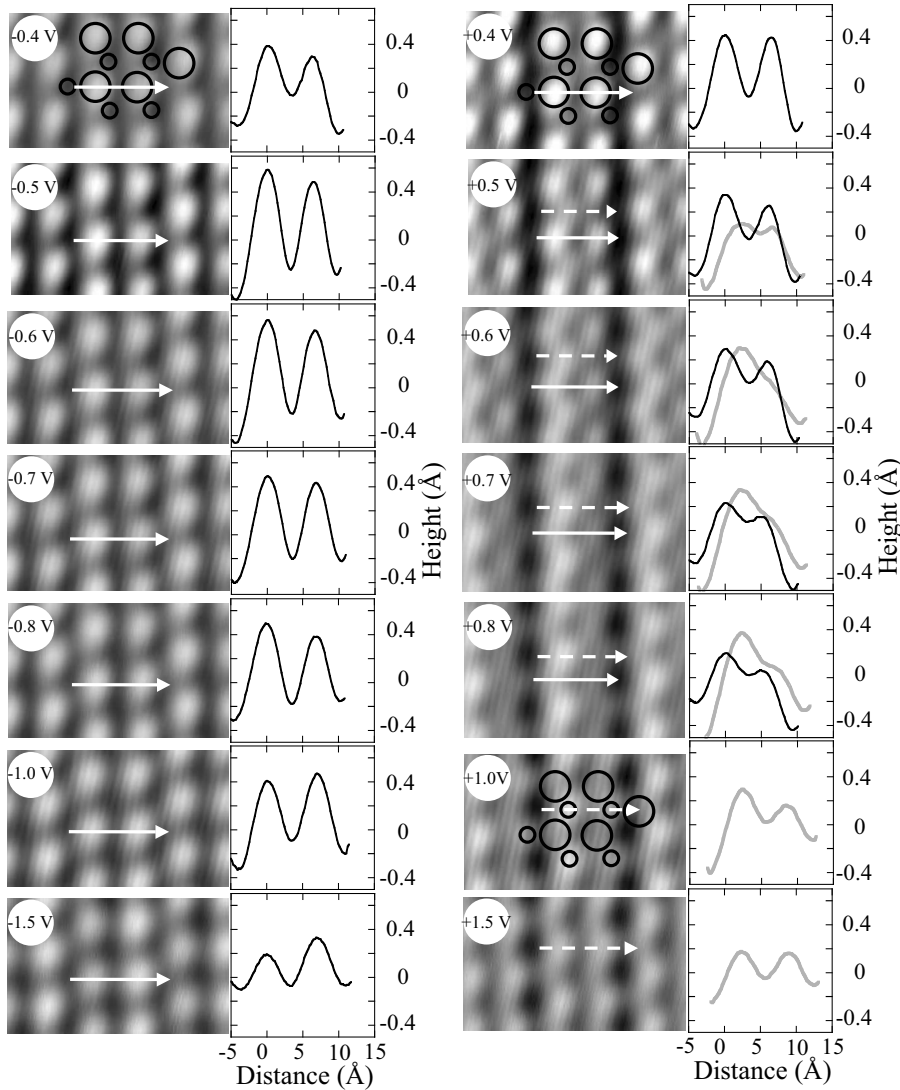


FIG. 4. Empty- and filled-state STM images recorded at different tip voltages. Line profiles across rest atoms (gray curves) and adatoms (black curves) are shown to illustrate the differences in apparent heights between the two types of rest atoms (R_T, R_R) and adatoms (A_T, A_R). All images were recorded with a constant tunneling current of 0.1 nA. Larger circles correspond to adatom positions, while smaller circles correspond to rest atom sites.

come brighter than the adatoms. As the positive tip voltage is increased, the rest atoms become dominant in the image while the adatoms become less visible which is noticeable already at +0.7 V. The inequivalence of the two types of rest atoms is evident in the +0.6 to +1.0 V images. The rest atom inside the rectangular subunit cell (R_R) is brighter as compared to the one inside the triangular subunit cell (R_T). This inequivalence becomes less pronounced at +1.5 V. The inequivalence is apparent from the line profiles passing through the adatoms and the rest atoms. The reversal of the brightness of the two adatoms in the empty-state images and the change in relative brightness of the two rest atoms in the filled-state images imply that the inequivalence of the two types of adatoms/rest atoms, as observed by STM, is not only due to geometric differences but has also an electronic origin. As a consequence of the inequivalence, one can expect that the charge transfer from the two types of adatoms to the two types of rest atoms is uneven.

Based on our electronic structure calculations we have generated simulated STM images of the Ge(111) $c(2 \times 8)$ surface (see Fig. 5). The empty-state images mainly show the adatoms, while the filled-state images show a variation in contrast for both adatoms and rest atoms. At -0.4 and

-0.6 V, the two types of adatoms appear virtually identical, while at -1.0 V they appear inequivalent; i.e., the A_R type is slightly brighter than A_T . This result is in agreement with the experimental STM images where the A_R adatoms become dominant at -1.0 V and the difference is quite clear at -1.5 V. In the simulated images of the filled states, adatoms appear higher at lower voltage as observed in the +0.4 V image. At +0.5 V, the rest atoms dominate the simulated image as well as in the +0.7 and +1.0 V images. Note that the R_R type is significantly brighter than the R_T type at +0.5 V and that the brightness becomes more equal at higher voltages. This is in excellent agreement with the experimental STM results. The theory predicts that the adatom brightness should increase when the voltage is increased as is evident in the +1.5 V simulated image. This increase in the adatom brightness was not observed in our experimental STM images obtained at +1.5 V, but the increase in the adatom brightness has in fact been observed in the filled-state images at +2.0 V.²¹ A set of simulated, bias-dependent, STM images of the Ge(111) $c(2 \times 8)$ surface, based on a Ge tip, was presented in a paper by Paz and Soler.²² The discussion of the results in the paper is very short, but by inspecting the theoretical STM images in Ref. 22 one can conclude

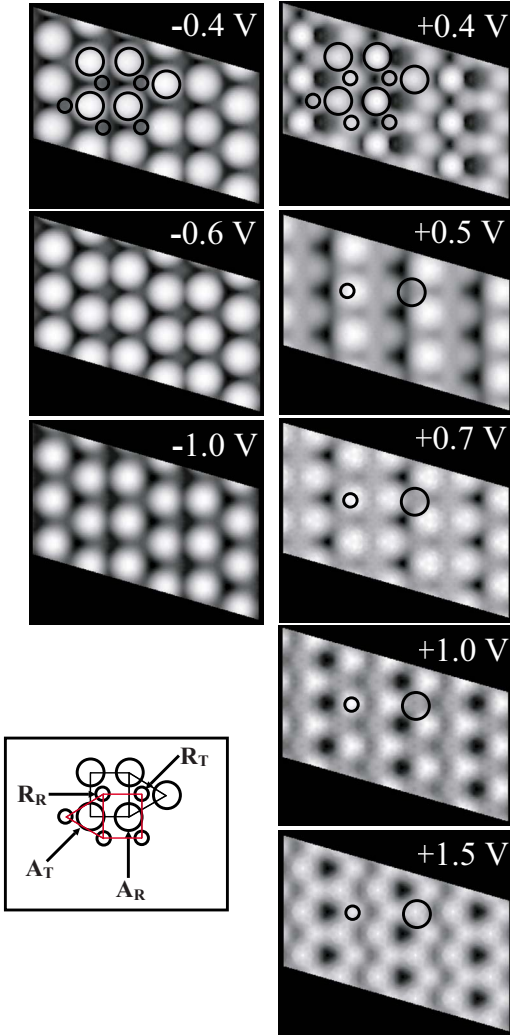


FIG. 5. (Color online) Simulated empty- and filled-state STM images of the Ge(111)c(2×8) surface at different tip voltages. A schematic diagram is shown to illustrate the positions of the different types of adatoms (A_T, A_R) and rest atoms (R_T, R_R).

that the general bias-dependent changes are similar to what we find in our simulated images. The adatoms are dominating the empty-state images, while the filled-state images show more variation with bias voltage. At the larger biases the adatoms dominate, but as the bias is decreased the rest atoms become dominating. At the lowest biases the adatom contribution starts to increase as in our simulated images (see Fig. 5). The inequivalence between the R_T and R_R rest atoms that is evident in the +0.5 V image in Fig. 5 can also be found by careful inspection of the simulated images of Ref. 22.

B. ARPES results and calculated surface bands

Figure 6 shows angle-resolved photoemission spectra of the Ge(111)c(2×8) surface recorded with a photon energy of 21.2 eV for various emission angles, θ_e , along the $[10\bar{1}]$ azimuth. Within 2 eV below E_F , seven distinct states were observed and they are labeled A1, A2, A2', A3, A4, A4', and

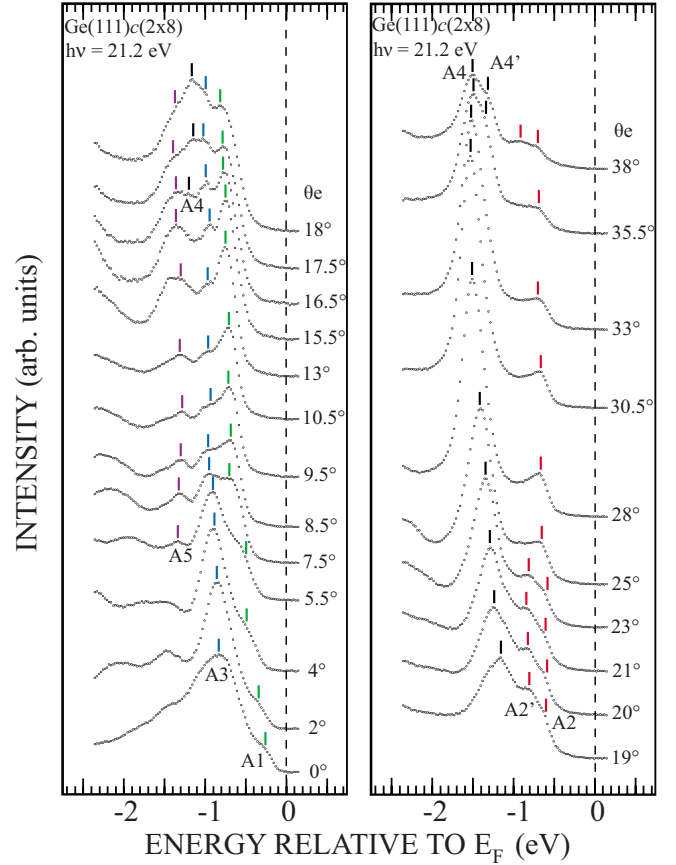


FIG. 6. (Color online) ARPES spectra of the Ge(111)c(2×8) surface recorded with a photon energy of 21.2 eV at 100 K for various emission angles along the $[10\bar{1}]$ azimuth. Different color markers are used to distinguish between surface states.

A5. These states represent a more detailed picture of the surface band structure of Ge(111)c(2×8) than presented in previous studies. This motivates a thorough investigation of the origins of these states. A1 lies at around -0.25 eV relative to E_F at normal emission, and it has dispersed to -0.7 eV at an emission angle of 18° . A1 has become a distinct peak at $\theta_e = 8.5^\circ$. It increases in intensity up to $\theta_e = 15.5^\circ$, and then it becomes a broader peak at the emission angles of 17.5 and 18° . A2 appears as a shoulder at $\theta_e = 19^\circ$ with an energy position of -0.6 eV, and it has dispersed slightly to -0.7 eV at $\theta_e = 38^\circ$. Another structure, A2' at around -0.8 eV, also appears at $\theta_e = 19^\circ$, and it is visible up to an emission angle of 23° with almost no dispersion. For higher emission angles the peak positions cannot be clearly identified except at the highest emission angle, $\theta_e = 38^\circ$, where it is found at around -0.9 eV. A3 is centered at around -0.8 eV at normal emission and disperses to -1.0 eV at $\theta_e = 18^\circ$ but can no longer be identified at 19° . A4 appears at $\theta_e = 16.5^\circ$ and is positioned around -1.2 eV. This structure has an intensity maximum at $\theta_e = 30.5^\circ$, and it disperses down to -1.5 eV at $\theta_e = 38^\circ$. A shoulder, A4', develops on the low binding energy side of A4 at higher emission angles. The position of A4' is about -1.4 eV at $\theta_e = 35.5^\circ$ and 38° . Finally, the structure A5 lies at around -1.3 eV and has dispersed to -1.5 eV at the emission angle of 18° .

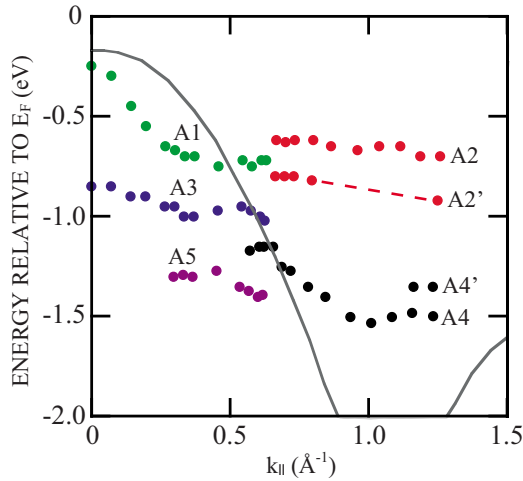


FIG. 7. (Color online) Energy dispersions, $E(k_{\parallel})$, of the different surface states observed on $\text{Ge}(111)c(2 \times 8)$ along the $[10\bar{1}]$ azimuth. Different colors are used to distinguish between the different surface-state bands (A1–A5). The solid line shows the upper edge of the bulk band structure projected onto a 1×1 SBZ.

In Fig. 7, the energy dispersions of the surface states have been plotted as a function of the wave-vector component parallel to the surface, k_{\parallel} . A comparison of the energy dispersions of our work and that of Aarts *et al.*¹⁰ is presented in Fig. 8. In the comparison of the data, a difference of 0.17 eV given by Guichar *et al.*²³ was assumed between E_F and the VBM. As mentioned above, seven surface-state bands can be clearly distinguished labeled as A1, A2, A2', A3, A4, A4', and A5; while in Ref. 10 four surface states were identified, namely, S1, S2, S3, and S4 as shown in Fig. 8. The band S1 corresponds to A1, A2, and A2'. There is a clear splitting into two bands at around $k_{\parallel} = 0.6 \text{ \AA}^{-1}$ in our photoemission spectra that we label A2 and A2'. The dashed part of the A2' dispersion indicates the presence of the structure in the spectra but that the energy positions cannot be accurately deter-

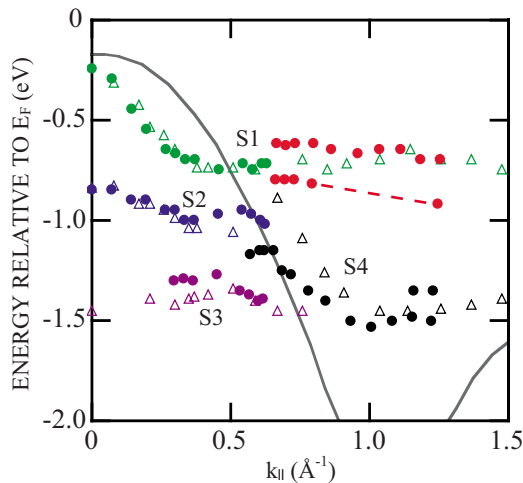


FIG. 8. (Color online) As Fig. 7 but including data from Aarts *et al.* (Ref. 10) shown by unfilled triangles (S1–S4). When plotting the data from Ref. 10, a value of 0.17 eV was assumed for the difference between E_F and VBM.

mined. Our A3 corresponds to the S2 band that was associated to rest atom dangling-bond states in the previous studies. The band S4 in Ref. 10, observed as two bands A4 and A4' in our case, was associated to back-bond states. Finally, our A5 structure seems to correspond to the S3 state of Ref. 10. Our dispersion curves agree fairly well with those of the previous study except for some important differences. The splitting into the A2 and A2' bands and the A4 and A4' splitting have not been reported before. The split observed between the A2 and A2' bands will play an important role in the discussion of the data in relation to the STM images obtained from the surface as well in relation to the calculated surface band structure.

The origins of some of the surface-state bands have not been fully resolved in the previous studies of the $\text{Ge}(111)c(2 \times 8)$ surface. Here we have combined experimental (STM and ARPES) and theoretical results in an effort to determine the possible origins of these surface bands. For the first time, band-structure calculations are presented for the full periodicity of the $\text{Ge}(111)c(2 \times 8)$ unit cell in this paper. Previous theoretical studies have been limited to first-principles calculations of the surface charge density⁵ and have often been done on the hypothetical $\text{Ge}(111)2 \times 2$ structure.²⁴ Figure 9 shows a superposition of a selection of our theoretical and experimental band structures. The experimental values have been shifted by 0.25 eV to obtain better agreement with theoretical values. Three differently oriented domains of the $c(2 \times 8)$ reconstruction are always present on the surface. Due to the symmetry of the (111) surface, they will differ by a 120° rotational angle. The experimental dispersion curves along a $[10\bar{1}]$ type of azimuth will therefore be a superposition of data from one $\bar{\Gamma}-\bar{K}$ and two $\bar{\Gamma}-\bar{K}'$ directions that represent different lines in the $c(2 \times 8)$ SBZ as illustrated by the inset in Fig. 9. The theoretical calculations of the surface band structure were done for the $\bar{\Gamma}-\bar{K}$ and $\bar{\Gamma}-\bar{K}'$ directions separately, and the result is plotted in Fig. 9. Since the experimental data cannot be separated into the $\bar{\Gamma}-\bar{K}$ and $\bar{\Gamma}-\bar{K}'$ contributions, we just plot the experimental data in both directions in Fig. 9. Note that the $\bar{\Gamma}-\bar{K}'$ direction is probed twice compared to $\bar{\Gamma}-\bar{K}$ which means that it is expected to dominate the experimental data. The experimental data points are shown by dots, while the theoretical energy values are shown as rectangles. The band-structure calculation generates a large number of bands due to the large size of the unit cell. In order to make a meaningful comparison we have only plotted the bands that we can clearly identify as surface related or that are of special relevance to the comparison with the photoemission data. In order to facilitate an easier comparison between experimental and theoretical energy bands as well as between experimental and simulated STM images, the subscript “theo” is used for the energies derived from the band-structure calculations and for the bias voltages of the simulated STM images, while the experimental values appear without any subscript.

The two bands above E_F , resulting from the calculation, are derived from the adatoms of the $c(2 \times 8)$ structure. Both of the unoccupied bands have a varying degree of A_T and A_R adatom character along the $\bar{\Gamma}-\bar{K}$ and $\bar{\Gamma}-\bar{K}'$ lines. The varia-

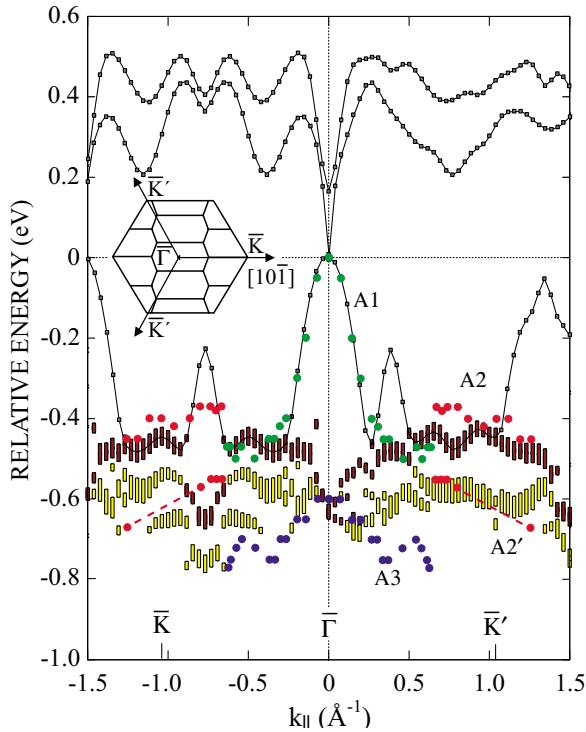


FIG. 9. (Color online) Comparison between experimental dispersions A1, A2, A2', and A3 (filled circles) and the theoretical surface bands (rectangles) in the corresponding energy range. The brown rectangles show R_R -derived rest atom states, while the yellow rectangles correspond to R_T -derived rest atom states. The heights of the rectangles are proportional to the ratio between the band decomposed charged density and the charge density of the whole system at each k_{\parallel} point. The presence of two split rest atom bands is obvious in the theoretical surface band structure. The two bands that are located above 0 eV are adatom derived. The experimental data points are shown relative to the highest energy position of A1.

tion is, however, relatively small, and it is therefore not possible to make a one-to-one match between the two bands and the two types of adatoms. This is in agreement with the theoretical study by Takeuchi *et al.*⁵ where they identified two adatom states (s8 and s9 in Ref. 5) of which both showed an even charge density on the two types of adatoms.

The uppermost occupied band from the calculation has a quite steep dispersion near $\bar{\Gamma}$. This band is not adatom or rest atom dominated but originates instead from lower layers, i.e., layers below the adatoms and the rest atoms. In Ref. 5, two overlapping states were reported (s6 and s7) just below E_F at $\bar{\Gamma}$ that are most likely of the same origin as our band. These states were not dangling bond like but were instead characterized as back-bond states mostly localized in the first bilayer, with some weight in the second bilayer. These states were reported to be very delocalized, both in the planar and vertical directions, which suggests a large dispersion as we actually find in our band-structure calculation. The A1 band, which has dispersed downward by ~ 0.5 eV at $k_{\parallel} \approx 0.4 \text{ \AA}^{-1}$, is plotted using green dots. We find an almost perfect agreement between the experimental data points and the calculated band, and we therefore identify the A1 band

with the states distributed a few layers down. This resolves the problem of how to interpret the S1 structure of Ref. 10 as was discussed in that paper.

Filled-state STM images in Fig. 4 show that at lower voltages, such as 0.4 and 0.5 V, the adatoms dominate because they are physically higher as compared to the rest atoms and there is no strong electronic effect from the rest atom states since they are located at higher binding energies as discussed in the coming paragraph.

In the energy region from -0.4_{theo} to -0.8_{theo} eV we find calculated bands that originate from the two types of rest atoms in the $c(2 \times 8)$ cell. They are basically split into two major bands separated by 0.1–0.2 eV. The upper band (brown rectangles) corresponds to the R_R rest atoms and the lower (yellow rectangles) to the R_T rest atoms. The split between the R_R and the R_T derived bands agrees quite well with the split that we have observed between the experimental A2 and A2' bands beyond $k_{\parallel} \approx 0.65 \text{ \AA}^{-1}$. In the filled-state STM images (Fig. 4); R_R is the first of the rest atoms to show up. It appears clearly at 0.6 V and is brighter than R_T in the 0.7–1.0 V images. The appearance of R_R at 0.6 V corresponds nicely with the energy position of the A2 band that is found in the energy range of 0.6–0.7 eV below E_F . The simulated STM images (Fig. 5) show the same trend with respect to the appearance of the R_R and the R_T types of rest atoms. At 0.4_{theo} V the simulated STM image is dominated by the adatoms since the bias is too small for a contribution from the rest atom dangling-bond states. At 0.5_{theo} V there is a strong contribution from the upper rest atom band and the R_R atoms dominate the simulated STM image. In the 0.7_{theo} and 1.0_{theo} V images, to which both the R_R and the R_T states contribute, the two types of rest atoms have a similar brightness. The rest atom inequivalence was also observed in the STM study performed by Lee *et al.*²⁵ and Hirschorn *et al.*⁴ on the Ge(111)c(2×8) surface at small negative sample voltages (-0.5 – -0.7 V). Based on the comparison between the experimental and theoretical results we conclude that the upper A2 band corresponds to the R_R rest atom dangling bonds and that the lower A2' band originates from the dangling bonds of the R_T rest atoms.

A similar type of split has been reported for the Si(111)7×7 surface, but in that case it is related to the dangling-bond orbitals on the adatoms that are partially occupied on that surface. The twelve adatoms of the 7×7 surface can be divided into four groups, i.e., two on the faulted and two on the unfaulted half of the 7×7 unit cell. The inequivalence of the adatoms manifests itself as a ≈ 0.35 eV split of the adatom-derived surface-state band near E_F .²⁶

The experimental A3 band is within the range of the calculated rest atom states. A similar band was observed by Aarts *et al.*¹⁰ who suggested an interpretation in terms of dangling-bond states on rest atoms, based on the intensity dependence on the light incidence angle and by comparing to the previous STM studies of Si(111)7×7.¹¹ This identification is in principle supported by a comparison of A3 and the lower lying R_T states in Fig. 9. One should however note that A3 is only observed within the projected bulk band region and may therefore be influenced by bulk emission. Thus, the A3 structure in the photoemission spectra may contain several contributions and a suggestion to identify A3 with the R_T

rest atoms can only be tentative, based on the available data. Some further ideas about the origin of A3 can be gained from the first-principles calculations by Takeuchi *et al.*,⁵ where a surface state, s3, was found at approximately 1 eV below E_F corresponding to 0.75 eV in Fig. 9. It was described as a back-bond state with some charge density on the R_R rest atoms. Based on the calculated band structure in Fig. 9, there exist some R_R states that coincide with the experimental band A3 in the vicinity of the $\bar{\Gamma}$ point. This could be a possible explanation to the result by Takeuchi *et al.*⁵ that the s3 state has some charge density on the R_R rest atom. To summarize, we have to conclude that there is not enough information to make a positive identification of the A3 band.

Contrary to band A3, A4 band is only observed in the 1×1 projected bulk band gap which makes a surface-state interpretation more straightforward. Compared to earlier studies we observe a shoulder on the A4 structure at the emission angles of 35.5 and 38°, which suggests the presence of two bands, labeled A4 and A4'. The dispersion and position of A4 within the projected band gap (see Fig. 7) are very similar to the adatom back-bond band on Si(111)7×7 which suggests the same origin. The split that we observe may result from a difference in the back-bond states of the A_T and A_R adatoms. In contrast to the rest atom case, we were not able to extract any bands with a strong back-bond character from our calculations to support our assignment. Apart from the comparison with Si(111)7×7 we find support for the back-bond interpretation in Ref. 5 where two states, s1 and s2, were found in the energy range corresponding to A4 and A4'. These states were assigned as first-layer dangling-bond states coupled to p_x, p_y adatom orbitals, and there was a small separation between the two states in qualitative agreement with the experimentally observed splitting.

Finally, our A5 band that corresponds to S3 in Ref. 10 was discussed as due to adatom structures on the Ge(111) surface in that paper. We can just conclude that we observe features in the photoemission spectra that seem to correspond to their S3 state, but we have no further information about the origin of this state.

IV. SUMMARY

In this study we have combined experimental and theoretical results to identify the origins of various surface-state bands on Ge(111)c(2×8). A total of seven surface bands was identified in the photoemission data, and the origins were discussed. The main results are: (i) we have identified the uppermost surface band A1 as originating from layers below the adatoms and rest atoms. This resolves the puzzle of why there is a band close to E_F although the adatom dangling bonds are empty. (ii) We have identified the contributions from the rest atoms, and we found a split between the R_T and R_R rest atom bands both experimentally and theoretically. The magnitude of the split compares nicely between experiment and theory. (iii) A split was also observed for the surface band assigned to back-bond states, but in this case just at higher emission angles. (iv) We find excellent agreement between experimental bias-dependent STM images and corresponding simulated STM images which strengthens the conclusions regarding the origins of the surface-state bands.

ACKNOWLEDGMENT

This work was supported by the Swedish Research Council.

*Present address: Department of Geography, King's College London, Strand, London WC2R 2LS, England, United Kingdom.

†Present address: Department of Physics, Karlstad University, S-651 88 Karlstad, Sweden.

¹D. J. Chadi and C. Chiang, Phys. Rev. B **23**, 1843 (1981).

²R. J. Phaneuf and M. B. Webb, Surf. Sci. **164**, 167 (1985).

³R. S. Becker, B. S. Swartzentruber, J. S. Vickers, and T. Klitsner, Phys. Rev. B **39**, 1633 (1989).

⁴E. S. Hirschorn, D. S. Lin, F. M. Leibsle, A. Samsavar, and T. C. Chiang, Phys. Rev. B **44**, 1403 (1991).

⁵N. Takeuchi, A. Selloni, and E. Tosatti, Phys. Rev. Lett. **69**, 648 (1992).

⁶R. D. Bringans and H. Höchst, Phys. Rev. B **25**, 1081 (1982).

⁷T. Yokotsuka, S. Kono, S. Suzuki, and T. Sagawa, J. Phys. Soc. Jpn. **53**, 696 (1984).

⁸J. M. Nicholls, G. V. Hansson, R. I. G. Uhrberg, and S. A. Flodström, Phys. Rev. B **33**, 5555 (1986).

⁹R. D. Bringans, R. I. G. Uhrberg, and R. Z. Bachrach, Phys. Rev. B **34**, 2373 (1986).

¹⁰J. Aarts, A. J. Hoeven, and P. K. Larsen, Phys. Rev. B **37**, 8190 (1988).

¹¹R. J. Hamers, R. M. Tromp, and J. E. Demuth, Phys. Rev. Lett.

56, 1972 (1986).

¹²F. Owman, Ph.D. thesis, Linköping University, 1996.

¹³G. Kresse and J. Hafner, Phys. Rev. B **47**, 558 (1993); Phys. Rev. B **49**, 14251 (1994).

¹⁴G. Kresse and J. Furthmüller, Comput. Mater. Sci. **6**, 15 (1996).

¹⁵G. Kresse and J. Furthmüller, Phys. Rev. B **54**, 11169 (1996).

¹⁶G. Kresse and D. Joubert, Phys. Rev. B **59**, 1758 (1999).

¹⁷P. E. Blöchl, Phys. Rev. B **50**, 17953 (1994).

¹⁸N. Takeuchi, A. Selloni, and E. Tosatti, Phys. Rev. B **51**, 10844 (1995).

¹⁹J. Tersoff and D. R. Hamann, Phys. Rev. Lett. **50**, 1998 (1983); Phys. Rev. B **31**, 805 (1985).

²⁰T. Klitsner and J. S. Nelson, Phys. Rev. Lett. **67**, 3800 (1991).

²¹J. R. Osiecki and R. I. G. Uhrberg (unpublished).

²²O. Paz and J. M. Soler, Phys. Status Solidi B **243**, 1080 (2006).

²³G. M. Guichar, G. A. Garry, and C. A. Sébenne, Surf. Sci. **85**, 326 (1979).

²⁴D. Drakova and G. Doyen, Prog. Surf. Sci. **46**, 251 (1994).

²⁵G. Lee, H. Mai, I. Chizhov, and R. F. Willis, J. Vac. Sci. Technol. A **16**, 1006 (1998).

²⁶R. I. G. Uhrberg, T. Kaurila, and Y.-C. Chao, Phys. Rev. B **58**, R1730 (1998).